

Site-Directed Mutagenesis as a Tool for Molecular Modeling of Cytochrome P450 2B1[†]

Grazyna D. Szklarz,* You Ai He, and James R. Halpert

Department of Pharmacology and Toxicology, College of Pharmacy, University of Arizona, Tucson, Arizona 85721

Received April 26, 1995; Revised Manuscript Received July 7, 1995[®]

ABSTRACT: Prompted by our previous homology model of cytochrome P450 2B1 based on the 3-D structure of P450cam [Szklarz, G. D., Ornstein, R. L., & Halpert, J. R. (1994) *J. Biomol. Struct. Dyn.* 12, 61–78], we constructed 11 new site-directed mutants at positions 100, 111, 205, 209, 291, 477, and 480 and expressed the enzymes in *Escherichia coli*. The mutations at positions 209, 477, and 480 affected androstenedione and progesterone hydroxylation as predicted by the model. For example, the Ile-477 → Ala and Ile-480 → Ala mutants retained ≤5% activity with androstenedione and progesterone but were active with benzphetamine, whereas the Leu-209 → Ala mutant catalyzed 21-hydroxylation of progesterone. Mutations at the other positions, i.e., 100, 111, 205, and 291, did not change enzyme activity, contrary to predictions. Therefore, an improved molecular model of cytochrome P450 2B1 was constructed. An alignment of the P450 2B1 sequence with P450 BM-3, P450cam, and P450terp was optimized using data from site-directed mutagenesis at 27 positions in various cytochromes P450 2B and docking of androstenedione into the active site of the known crystal structures. Because all three structures were found to be suitable templates for P450 2B1, the new model was formulated on the basis of the crystallographic coordinates of the three proteins using a consensus strategy, a modeling method based on distance geometry calculations. The new model provides a means to explain alterations in regio- and stereospecificity of steroid hydroxylation upon residue substitution at key amino acid positions, including positions 114, 206, 209, 290, 302, 363, 367, 477, 478, and 480 in P450 2B1.

Cytochromes P450 are a superfamily of heme-containing enzymes that catalyze the monooxygenation of a variety of substrates ranging from endogenous compounds such as steroids or prostaglandins to xenobiotics such as drugs and environmental pollutants (Guengerich, 1993). Many forms of P450¹ display broad substrate specificities, but individual isoforms often exhibit strict regio- and stereospecificity toward some substrates, e.g., steroids. In recent years, much effort has been devoted to understanding the structural basis for such specificity and to elucidation of structure–function relationships of these enzymes [e.g., Johnson (1992) and Korzekwa and Jones (1993)].

To date, four bacterial P450 structures have been solved by X-ray crystallography: P450cam (P450 101), a camphor hydroxylase from *Pseudomonas putida* (Poulos et al., 1985, 1987), P450 BM-3 (P450 102), a fatty acid monooxygenase from *Bacillus megaterium* (Ravichandran et al., 1993), P450terp (P450 108), an α -terpineol monooxygenase from *Pseudomonas* sp. (Hasemann et al., 1994), and P450eryF, a 6-deoxyerythronolide B hydroxylase from *Saccaropolyspora erithrea* (Cupp-Vickery & Poulos, 1995). Although these bacterial enzymes display low (15–20%) amino acid sequence identity with eukaryotic P450s, certain regions of the

sequence, such as the heme binding site, the oxygen binding site, and the site of interactions with redox partners, are highly conserved (Nelson & Strobel, 1988, 1989), implying conservation of structure. Furthermore, comparison of known structures indicates that the topology of all the enzymes is similar, especially in the heme binding core region (Hasemann et al., 1995; Cupp-Vickery & Poulos, 1995). Since none of the eukaryotic P450s has been crystallized, molecular models of various mammalian enzymes have been constructed (Vijayakumar & Salerno, 1992; Laughton et al., 1993; Koymans et al., 1993) to explain substrate specificity and to relate enzyme function to its structure.

Site-directed mutagenesis together with the concept of substrate recognition sites (Gotoh, 1992) has been successfully applied to identify residues responsible for substrate specificity in many cytochromes P450 of family 2. These key residues include residues 117, 209, and 365 in the mouse 2A subfamily (Lindberg & Negishi, 1989; Juvonen et al., 1991; Iwasaki et al., 1993), residues 114, 206, 290, 302, 363, 367, and 478 in 2B enzymes (Aoyama et al., 1989; Kedzie et al., 1991; He et al., 1992, 1994; Halpert & He, 1993; Luo et al., 1994; Hasler et al., 1994), residues 112–115, 301, 359, and 364 in the 2C subfamily (Imai & Nakamura, 1989; Kaminsky et al., 1992; Hsu et al., 1993; Straub et al., 1993a,b, 1994; Richardson & Johnson, 1994), and residue 380 in P450 2D1 (Matsunaga et al., 1990). Since structure–function relationships of rat cytochrome P450 2B1 have been of major interest in our laboratory in the last few years (Kedzie et al., 1991; He et al., 1992, 1994; Halpert & He, 1993; Luo et al., 1994), we recently developed a three-dimensional model of this enzyme based on the crystal

[†] Supported by Grant ES03619 from the National Institutes of Health.

* To whom correspondence should be directed: telephone, (520) 626-4489; FAX, (520) 626-2466; E-mail, Szklarz@tonic.pharm.arizona.edu.

¹ Abbreviations: P450, cytochrome P450; CHAPS, 3-[(3-cholamidopropyl)dimethylammonio]-1-propanesulfonate; HEPES, 4-(2-hydroxyethyl)-1-piperazineethanesulfonic acid; TLC, thin-layer chromatography; SCRs, structurally conserved regions; SRS, substrate recognition site.

structure of P450cam (Szklarz et al., 1994). The model correctly assigned positions for 9 out of 10 2B1 residues studied by site-directed mutagenesis and allowed a plausible explanation of some of the changes in regio- and stereospecificity caused by certain amino acid substitutions. Furthermore, the model indicated other residues which may be important for enzyme activity.

Therefore, in the present investigation, we constructed single mutants of P450 2B1 at positions 100, 111, 205, 209, 291, 477, and 480, which were predicted by the model to be important for steroid hydroxylation. The mutant proteins were expressed in *Escherichia coli* and assayed with androstenedione and progesterone as substrates. An improved model of P450 2B1 was built on the basis of three known crystal structures, P450cam, P450 BM-3, and P450terp, using consensus modeling methods. We have utilized a novel approach to refine the sequence alignment using data from site-directed mutagenesis in combination with docking of substrate into the active site of known structures and estimating the feasibility of interactions between the substrate and key residues. Our new model possesses coordinates which are weighted averages of all reference proteins and is in agreement with site-directed mutagenesis data for cytochromes P450 2B.

EXPERIMENTAL PROCEDURES

Materials. Primers for site-directed mutagenesis and DNA sequencing were obtained from the University of Arizona Macromolecular Structure Facility (Tucson, AZ). The pKK233-2 *E. coli* expression plasmid was purchased from Pharmacia (Alameda, CA), and Topp3 cells were from Stratagene (La Jolla, CA). Growth media for *E. coli* were obtained from Difco (Detroit, MI). Restriction endonucleases and DNA modification enzymes were purchased from GIBCO-BRL (Grand Island, NY). Androstenedione, benzphetamine, NADPH, dilauroyl-L-3-phosphatidylcholine (DLPC), and CHAPS were obtained from Sigma (St. Louis, MO). [^{14}C]Androstenedione and [^{14}C]progesterone were purchased from DuPont-New England Nuclear (Boston, MA). TLC plates [silica gel, 250 μM , Si 250 PA (19C)] were obtained from J. T. Baker Inc. (Phillipsburg, NJ). HEPES was purchased from CalBiochem Corp. (La Jolla, CA). All other reagents and supplies not listed were obtained from standard sources.

Site-Directed Mutagenesis and Expression of P450 Enzymes in *E. coli*. Wild-type P450 2B1 cDNA was introduced into the pKK233-2 expression vector as described previously (John et al., 1994). The second codon had been modified from GAG to GCT to increase expression in *E. coli* (John et al., 1994). The USE mutagenesis kit from Pharmacia (Piscataway, NJ) was used for the introduction of specific base changes into the P450 2B1 cDNA to produce the following single mutants of P450 2B1: Thr-100 \rightarrow Lys, Tyr-111 \rightarrow Phe, Thr-205 \rightarrow Ser, Leu-209 \rightarrow Ala, Ser-291 \rightarrow Thr, Ile-477 \rightarrow Ala, and Ile-480 \rightarrow Ala. The unique restriction site eliminated in the process of mutagenesis was a *SalI* site in the vector. The substitution of Ile with Leu or Val at positions 477 and 480 was carried out by PCR. The mutants were constructed in the pKK233-2 vector by replacing a 380 bp *BglII* fragment from the second codon-modified wild type with the corresponding fragment from the mutants. All mutated codons were confirmed by double-

stranded sequencing using a Sequenase 2.0 kit from the U.S. Biochemical Corp. (Cleveland, OH). Plasmids containing the P450 2B1 wild-type and mutant cDNAs were transformed to Topp3 cells. *E. coli* were grown and CHAPS-solubilized membranes prepared as described previously (John et al., 1994; He et al., 1995).

Substrate Metabolism by Expressed P450 2B1 and 2B1 Mutants. The assays of steroid hydroxylase activity were performed as described earlier (John et al., 1994; He et al., 1995), except that 5 pmol of P450 and 17.5 pmol of rat liver NADPH-P450 reductase were used in each enzymatic reaction. Androstenedione and progesterone metabolites were then resolved on TLC plates (Hasler et al., 1994; John et al., 1994; He et al., 1995). 21-Hydroxyprogesterone was identified by autoradiography through comparison with the standard in three different development systems: benzene/ethyl acetate/acetone (10:1:1 v/v/v), chloroform/ethyl acetate/ethanol (20:5:1 v/v/v), and ethyl acetate/*n*-hexane/acetic acid (16:8:1 v/v/v). Identification of the metabolite as 21-hydroxyprogesterone was further confirmed by atmospheric pressure chemical ionization–tandem mass spectral analysis with a Finnigan TSQ 7000 instrument (Finnigan MAT, San Jose, CA). Collision-induced dissociation of the $[\text{M} + \text{H}]^+$ ion at m/z 331 yielded principal fragments at m/z 109 and m/z 97. The observed product ion spectrum was identical to that produced from a 21-hydroxyprogesterone standard under identical conditions. Benzphetamine *N*-demethylation was measured by the formation of formaldehyde (Nash, 1953), as detailed elsewhere (He et al., 1995).

Molecular Modeling. General. The crystallographic coordinates of P450cam were obtained from the Brookhaven Protein Data Bank (Poulos et al., 1987), and those of P450 BM-3 (Ravichandran et al., 1993) and P450terp (Hasemann et al., 1994) from Dr. Julian A. Peterson, University of Texas Southwestern Medical Center at Dallas. The P450 2B1 structure was modeled using INSIGHTII/CONSENSUS software (Biosym Technologies, San Diego, CA) on a Silicon Graphics workstation. Energy minimization and molecular dynamics calculations were performed using the DISCOVER program (Biosym Technologies, San Diego) with the consistent valence force field. The parameters for heme and ferryl oxygen were as described by Paulsen and Ornstein (1991, 1992).

Sequence Alignment. To align the P450 2B1 sequence to those of P450cam, P450 BM-3, and P450terp, we utilized the structure-based alignment of these three proteins, obtained courtesy of Dr. Julian A. Peterson, University of Texas Southwestern Medical Center at Dallas. The starting point for this multiple alignment was the previously published alignment 2 between P450 2B1 and P450cam (Szklarz et al., 1994), which was refined manually with HOMOLOGY (Biosym Technologies, San Diego). Structurally conserved regions (SCRs) were determined on the basis of scores of Dayhoff's mutation matrix and the Engleman and Steitz hydrophobicity index for each pair of sequences (i.e., 2B1–P450cam, 2B1–P450 BM-3, and 2B1–P450terp). Additionally, we utilized data from site-directed mutagenesis of cytochromes P450 2B in conjunction with docking of androstenedione, a substrate of P450 2B1, into the active site of P450cam, P450 BM-3, and P450terp to evaluate and further optimize the alignment. The procedure is described in Results.

Table 1: Metabolism of Androstenedione and Progesterone by Wild-Type and Mutant P450 2B1 Expressed in *E. coli*^a

	androstenedione					progesterone		
	15 α -OH	16 β -OH	16 α -OH	total activity	%	16 β :16 α	16 α -OH ^b	%
WT ^c	0.2	22.4	2.8	25.5	100	8.0	6.7	100
T100K	0.1	12.9	1.3	14.3	56	10.1	3.2	48
Y111F	0.1	12.7	1.6	14.4	57	7.7	1.8	27
T205S	0.2	14.4	2.2	16.8	66	6.6	7.6	113
L209A ^d	0.1	14.8	3.2	18.1	71	4.7	13.7 ^d	204
S291T	0.2	17.3	2.8	20.2	79	6.2	10.0	149
I477A	0.01	0.4	0.04	0.45	1.2	10.0	0.3	5
I477V	0.1	12.5	1.1	13.7	54	11.3	1.2	18
I477L	0.2	12.2	1.2	13.5	53	10.2	5.0	75
I480A	0.01	0.1	0.02	0.13	0.5	5.0	0.2	3
I480V	0.2	12.3	1.7	14.2	56	7.2	1.5	22
I480L	0.4	25.9	3.4	29.7	117	7.5	1.5	22

^a All values reported are derived from duplicate incubations performed as described in Experimental Procedures and are expressed in nmol of product min⁻¹ (nmol of P450)⁻¹. ^b 16 α -Hydroxyprogesterone is a major metabolite produced by P450 2B1 (Swinney et al., 1987). ^c WT, wild type.

^d This mutant was found to produce 21-hydroxyprogesterone, ca. 0.5 nmol min⁻¹ (nmol of P450)⁻¹, which was not detected in the case of the wild-type enzyme.

Modeling the P450 2B1 Structure. After the SCRs were determined, coordinates of the model were calculated using CONSENSUS. This program employs distance geometry calculations which allow the use of several reference proteins simultaneously. Within SCRs, coordinates of the model are weighted averages of coordinates of reference proteins. Three different structures obtained were evaluated by docking androstenedione into the active site in a manner similar to that employed in optimizing the sequence alignment. The best structure, structure 1, was further modified using the BIOPOLYMER program (Biosym Technologies, San Diego) to achieve the best agreement with experimental data. Modified regions were then minimized, side chains first and then all atoms, using the steepest descent method and harmonic potential to a maximum gradient of 5 kcal mol⁻¹ Å⁻¹. The nonbond cutoff was 8 Å and the dielectric constant was 1.0. Some loops, e.g., the B'-C loop, were optimized with one cycle of combined molecular dynamics and minimization, as described earlier (Szklaarz et al., 1994). The final refinement of the model involved minimization of the whole structure in the presence of water. Water molecules were from soaking the protein using a sphere of 25 Å and a layer of 3 Å. The minimization was thus performed on a protein-water association, using at first the steepest descent method until the gradient was less than 5 kcal mol⁻¹ Å⁻¹ and then conjugate gradients to a maximum of 1 kcal mol⁻¹ Å⁻¹ (Szklaarz et al., 1994). The model was verified with the Profiles-3D program (Biosym Technologies, San Diego), which measures the compatibility between the protein sequence profile and its 3-D profile (Bowie et al., 1991; Luthy et al., 1992).

Docking of the Substrate into the Active Site. The docking of the substrate had a double objective: (1) refinement of the sequence alignment and evaluation of initial CONSENSUS structures, as described above, and (2) explanation of specificity of substrate hydroxylation by P450 2B1. In both cases, the substrate was placed in a reactive binding orientation, with the oxidation site fixed at 5.6–6 Å from the heme iron and the C-H bond aligned with ferryl oxygen, heme iron, and sulfur of Cys-436, as described earlier (Szklaarz et al., 1994). This results in a hydrogen-bonding distance between ferryl oxygen and the hydrogen atom to be abstracted from the substrate. Two substrates, androstenedione and progesterone, were docked into the final

model. The oxidation site was fixed at C₁₆, C₁₅, or C₆ and, additionally, at C₂₁ for progesterone, with ferryl oxygen bound to the iron. Conformational analysis of progesterone was performed with the SEARCH COMPARE module of INSIGHTII. The nonbond interaction energy between the steroid and the protein, both electrostatic and van der Waals forces, was evaluated with the DOCKING module of the INSIGHTII package to find low-energy binding orientations. To optimize enzyme-substrate interactions, the steroid was fixed in a low-energy binding orientation and the residues in contact with the substrate (less than 4 Å distance) were minimized using the steepest descent method until the gradient was less than 5 kcal mol⁻¹ Å⁻¹ (Szklaarz et al., 1994). Since the conformational changes introduced were highly localized, the rms deviation upon minimization was in the range of 0.03–0.14 Å for the backbone and 0.08–0.26 Å for all atoms.

RESULTS

Catalytic Activities of P450 2B1 Mutants. Our earlier model of P450 2B1 (Szklaarz et al., 1994) based on the structure of P450cam indicated that several residues not previously studied may affect the activity of the enzyme. Therefore, to test that model, we constructed single mutants of P450 2B1 at various locations in the vicinity of the active site. The mutants were T100K in the B-C loop, Y111F in helix B', T205S and L209A in helix F, S291T in helix I, and I477A, I477V, I477L, I480A, I480V, and I480L in β -sheet 4 and the neighboring loop.² The mutants and the wild-type P450 2B1 were expressed in *E. coli*, a system which allows for high levels of expression (John et al., 1994). The expression levels of P450s in *E. coli* cultures were in the range of 140–330 nmol L⁻¹, and the solubilized membrane preparations were obtained with about 30% recovery, yielding about 50–100 nmol L⁻¹. The substrates used to verify enzymatic activities of P450 2B1 mutants were androstenedione and progesterone, shown to be metabolized efficiently by the enzyme in earlier studies [e.g., He et al.

² The last region was designated in our previous studies (Szklaarz et al., 1994) as sheet β -5 according to the nomenclature introduced by Poulos et al. (1985, 1987). In this paper, we use the nomenclature for the secondary structural elements proposed by Peterson and colleagues (Ravichandran et al., 1993; Hasemann et al., 1994, 1995).

(1992, 1994)]. The results for these two steroids are presented in Table 1. In the case of androstenedione, the most striking decrease in activity is observed with the I477A and I480A mutants, to about 1% or less of the wild-type activity. In contrast, the mutation of Ile at these positions to either Val or Leu does not cause such a major change. The I477A and I480A mutants also display $\leq 5\%$ of wild-type activities with progesterone. Therefore, these two mutants were also tested with another substrate, benzphetamine, to verify whether they are active enzymes. The Ile-477 \rightarrow Ala mutant metabolized benzphetamine at a rate of $11.3 \text{ nmol min}^{-1} \text{ nmol}^{-1}$ and the Ile-480 \rightarrow Ala mutant at a rate of $12.8 \text{ nmol min}^{-1} \text{ nmol}^{-1}$ compared with $33 \text{ nmol min}^{-1} \text{ nmol}^{-1}$ in the case of the wild-type enzyme. Another interesting mutant is L209A, which, in addition to increased rates of progesterone 16α -hydroxylation, forms the novel metabolite 21-hydroxyprogesterone at the rate of *ca.* $0.5 \text{ nmol min}^{-1} \text{ nmol}^{-1}$ (Table 1). This is in contrast to the wild-type enzyme, which hydroxylates progesterone mainly in the 16α -position (Swinney et al., 1987). Furthermore, 21-hydroxyprogesterone was not detected as a metabolite in the case of other mutants of P450 2B1 at positions 114, 206, 302, 363, 367, and 478 (Luo et al., 1994; He et al., 1995). Thus, position 209 seems to be unique in its ability to confer 21-hydroxylase activity toward progesterone in cytochrome P450 2B1 upon mutagenesis to alanine. Overall, major changes in steroid hydroxylase activity were observed upon mutations at three (209, 477, and 480) out of seven positions suggested by our previous model.

P450 Sequence Alignment and Model Building. To build a new model of P450 2B1, we used a structure-based alignment of P450cam, P450 BM-3, and P450terp. This alignment was refined by incorporation of the data from site-directed mutagenesis of cytochromes P450 of the 2B subfamily and docking of androstenedione into the active site. The underlying assumption is that key residues should be able to interact with the substrate.

The initial alignment established equivalence between 27 residues of P450 2B enzymes studied by site-directed mutagenesis (listed in Table 2) and appropriate residues of P450cam, P450 BM-3, and P450terp. The three crystal structures were then superimposed using heme as a basis, and those residues were displayed. Next, androstenedione was docked into the active site in a 16β -binding orientation and manually rotated along the $C_{16}-H_{16\beta}$ axis to place the molecule in the vicinity of residues of interest. The 16β -binding orientation was chosen because androstenedione is hydroxylated by P450 2B1 mainly in the 16β -position (Waxman, 1988). Docking of androstenedione made it possible to evaluate whether a given residue may interact with the substrate, as judged by its distance (less than 4 Å) and orientation with respect to the substrate.

The sequence refinement procedure may be illustrated by the example of the region at the end of helix F and the beginning of the F-G loop, containing residues 204, 205, 206, and 209 of P450 2B1. In that region, the structure of P450terp is quite different from those of P450cam and P450 BM-3, and no coordinates are available for the F-G loop since it is disordered in the crystal (Hasemann et al., 1994). Thus, only P450 BM-3 and P450cam were used to model this region and were included in the SCR, as shown in Figure 1. However, two alignment possibilities can be considered. In alignment A, Arg-204 of P450 2B1 aligns with Glu-183

Table 2: Residues Studied by Site-Directed Mutagenesis in P450 2B Enzymes and Their Equivalents in Crystal Structures of P450 BM-3, P450cam, and P450terp, According to the Alignment in Figure 1

secondary structure	2B1	BM-3	cam	terp	effect ^a (ref) ^b
$\beta 1-5-B'$ loop	T100	S72	P86	G75	— (a)
helix B'	I107	V78	A92	N83	— (b)
helix B'	Y111	A82	Y96	F87	— (a)
B'-C loop	I114	G85	I99	S101	+ (b, c, f, h)
E-F loop	D192	P170			— (d)
helix F	L199	M177	L177	M180	— (b)
helix F	E200	V178	K178	L181	— (b)
helix F	R204	D182	D182	Q185	— (b)
helix F/loop	T205	E183	Q183	D186	— (a)
helix F/loop	F206	A184	M184	F187	+ (e, f, g)
F-G loop	L209	K187	P187	V190	+ (a)
helix G	I234	F205	F193	F211	— (b)
helix G	K236	E207	E195	E214	— (f)
helix I	I290	Y256	R240	A259	+ (b, h)
helix I	S291	Q257	M241	Y260	— (a)
helix I	L292	I258	C242	Y261	— (b)
helix I	T302	T268	T252	T271	+ (f, g)
helix I	S303	T269	V253	T272	— (g)
K- $\beta 1-4$ loop	S360	W325	F292	T311	— (g)
K- $\beta 1-4$ loop	V363	A328	V295	V314	+ (b, e, f, g, h)
K- $\beta 1-4$ loop	I365				+ (h)
sheet $\beta 1-4$	V367	F331	D297	F317	+ (f, g)
sheet $\beta 4-1$	K473	K434	K392	V410	— (b, g)
$\beta 4-1-\beta 4-2$ loop	S475	E435	S393	T412	— (b)
$\beta 4-1-\beta 4-2$ loop	I477	L437	I395	F414	+ (a)
$\beta 4-1-\beta 4-2$ loop	G478	T438	V396	V415	+ (c, e, f, i, j)
sheet $\beta 4-2$	I480	K440	G398	G417	+ (a)

^a Alteration in activity upon mutation is designated with a (+) (key residues) and is represented by changes in the steroid hydroxylase profile and/or major decrease in activity (to $\leq 5\%$ wild type); no change in activity is denoted with a (—). This was studied in cytochromes P450 2B1, 2B4, 2B5, and 2B11. ^b References: a, present study; b, Hasler et al., 1994; c, Halpert & He, 1993; d, Zongshu Luo, unpublished data; e, Luo et al., 1994; f, He et al., 1995; g, He et al., 1994; h, Born et al., 1995; i, Kedzie et al., 1991; j, He et al., 1992.

of P450 BM-3 and Gln-183 of P450cam, Thr-205 of 2B1 is equivalent to Ala-184 in P450 BM-3 and Met-184 in P450cam, Phe-206 of 2B1 aligns with Met-185 of P450 BM-3 and Thr-185 of P450cam, and Leu-209 of P450 2B1 aligns with Leu-188 of P450 BM-3 and Asp-188 of P450cam. The alternative alignment B is shown in Figure 1, where residues 204, 205, 206, and 209 of P450 2B1 correspond to residues 182, 183, 184, and 187, respectively, of P450 BM-3 and P450cam. When androstenedione is docked into the crystal structures, both Met-184 and Thr-185 of P450cam and Ala-184 and Met-185 of P450 BM-3 are close to the substrate. However, site-directed mutagenesis data indicate that among residues 204, 205, 206, and 209 in P450 2B enzymes only one residue, Phe-206, should be able to interact with androstenedione (Tables 1 and 2). In alignment B, when residues 182, 183, 184, and 187 of P450cam and P450 BM-3 are displayed, only Met-184 of P450cam and Ala-184 of P450 BM-3, which correspond to Phe-206 of 2B1, are close to the substrate, in agreement with the data. Similar analysis was performed for other regions of the P450 2B1 sequence for which the mutagenesis data were available. The final alignment is shown in Figure 1, and the residues that have been studied in 2B enzymes and their equivalents in bacterial P450 structures are listed in Table 2.

The analysis of the superimposed crystal structures shows that the P450 fold is well preserved, as reported by Hasemann et al. (1995). Furthermore, the residues of P450 BM-3,

B1	: meptilllllallvgfllllvrghpksgnfp PPGPRPLP ilgn--llqldrqg LLNSFMQL Rekyg--- DVFTV hlg	71
BM3	: TIKEMPQPKTF GELKNLPLNTDK-- PVQALMKI ADeLG--- EIFKFE AP	45
CAM	: NLAPLP PHVPEHLVDFDMYNPSNLSAGV QEA WAVL QES NV-- PDLVW TRCN	59
TERP	: MDARAT IP EH IARTVILPQGYA---DDEVIPAFKWL RD EQ PLAM AHIE	46
	A 1-1	
B1	: p-rp VV MLCg TD TIKEALvggae DFS grgt-iavie PIFKEY -----gvifang---- erWKALRR FSLa	130
BM3	: G-RV TRYLSSQ RLIKEACDE--SRFDKNLS-- QALKFVR DFA-----GDGLFTSWTHEKN WKA HNILLP	105
CAM	: G-- GH WIATRG QL IREAYED-YRHSSECP-- FIPREAGE AY-----DFIPTSMDF-- PEQRQ FRALANQ	117
TERP	: GYD P MW IAT KHAD V M Q IGKQ-PGLFSNAEGSEILYD Q NE A FMR S ISGGCPHVIDSLTSMDF-- PTH TAYRGLTLN	119
	1-2 B 1-5 B' C	
B1	: tmrdfgmgkrsv EERI QE EAQ CLVEELrks-- QGAP Ldptflfq CITANI ICSIVfgerfd----ytdrqf LRL L	199
BM3	: SFSQ QAM KG--YHAM VD IAV Q LVQ K WERLNADEHIEVPE-DM TRLT LD TIG LCGFNYRFN-SFYRDQ PH PFIT SM	177
CAM	: VVGMPVVDK-- LENRI QELACSLIESLRP-- QGQC NFTEDYAE FPPIRIF MLLAGLPEED----- IPHL	177
TERP	: WFQ PAS IRK-- LEENIR RIA QASVQ RLLD F --D GEC DFMTDCALY YPLHV MTALGV PED D----- EPLM	180
	D 3-1 E	
B1	: ELFYR tfslsssfssqvfeffsgflkyfpgahrq ISKNLQ EILDY IGHIVE KHRatldpsapr DFID TYL irmEKE	275
BM3	: VRALDE AMNKLQ-----RANPD DPAY DENKR QFQ EDI KVMND LV DKI IAD RKAS GE--QSD DLL THMLN-- GKD	242
CAM	: KYLTDQ MT RPD -----GSMT FAEAK EALYD YLIPI IE QRRQ KP---GTDAISIVAN-- GQV	228
TERP	: LKLTQ DFFGVHEPDEQA---VAAP RQSA DEAARRFHETIATFYDYFNGFTVDRRSCP---KDD VMS LLAN-- SKL	247
	F G H 5-1	
B1	: ksnhh TEF HHENLMISLLS LF FAGTETSSTTLRYG FL MLK yP HA VEK VQKeidqvigshrlptlddrskmpy TDA	351
BM3	: -PETGEPLDDENIRYQ II TFLIAGHETT SGL LSFALYFLVKN PHV LQ AAE EAARVLVDP-VPSY KQV KQLKY VGM	316
CAM	: ---NGRPITSDEAK RC GLLLVGGLD TVN FLS SME FLAK SPE HRQELIERPER----- IPA	283
TERP	: ---DGN YID KYINAYYVAIATAGHDT SSSSG GA IIG LSRN PEQ ALAKSDPAL----- IPR	302
	5-2 I J	
B1	: VIHEI Q R Fsdlvpig VPH RVTK DTM Frg-YLLpk nTEV Y P ILSSALhdppqyf-dhpdsfnpehflangalkksea	425
BM3	: VLNEA LRLWPTAP-AFSLYAKEDTVLGGEYPLEKGDEL VL IP Q LHRDKTIWGD DVEE FRPERFENPSAI--PEHA	389
CAM	: ACEE LLRRFS LV --ADGRILTS DYEF HG-V Q LKKGD Q ILL PQ ML SGL DERENA-CPMHVDFSRQKVS-----	346
TERP	: LVDEA VRWTAPVK-SFMRTALADTEVRG- Q NIKR GDR IMLSY PSAN RDEEVFS-NPDEFDITRFPNR-----	366
	K 1-4 2-1 2-2 1-3 K'	
B1	: FMPF STGKRICLGE GI ARNEL FL FFTTIL QN FSVSshlapkdidl TPK esgig kIP pt YQ ICFsar	491
BM3	: FKP FGNG Q RACIG Q Q FAL HEAT LV LGM LKH FD FE DHT---NYELDIK-ETLTL KPE GF VV KAKSKKI PL GG	457
CAM	: HTT FGH SH LC L CG HL ARRE I IVTLKEWL TR IP DF SIA--PGAQ IQ HK-SGIVSGV QAL PLV DP ATT KAV	414
TERP	: HLG FGWGA HM CL G Q HL AK LE M KI FF EEL LP KL KS VEL S----G P RLVATNFVG G PK NV IR FT KA	428
	L 3-3 4-1 4-2 3-2	

FIGURE 1: Sequence alignment between P450 2B1, P450cam, P450 BM-3, and P450terp. Residues contained in helices and sheets of P450 2B1 are shown in capital letters, and each 10th residue is marked with a dot above the 2B1 sequence. Helices are indicated by letters and β -sheets by numbers below the sequences. Structurally conserved regions (SCRs) are shown in bold. In some cases, e.g., helix G, only two structures may have served as templates.

P450cam, and P450terp equivalent to key residues 290, 302, 363, 367, and 480 of P450 2B1 occupy similar coordinates in all three proteins and are able to interact with docked androstenedione (not shown). A similar situation is observed in the case of those P450 BM-3 and P450cam residues that correspond to key residues 206, 477, and 478 of P450 2B1. This led us to conclude that, basically, any of the P450 structures may be used for modeling of P450 2B1 due to high conservation of the core structural elements. We decided to use the Consensus modeling method, not previously used for modeling P450s, in which the coordinates of the model are weighted averages of the coordinates of the bacterial proteins and thus may better describe the 2B1 structure. In some regions, e.g., helix B' and the B'-C loop, the known proteins display high structural diversity, and the evaluation of the model was based solely on site-directed mutagenesis data in conjunction with docking of androstenedione, as described above.

The model of P450 2B1 is presented in Figure 2, showing the location of residues studied by site-directed mutagenesis.³ Key residues, i.e., those which affect regio- and stereospecificity of steroid hydroxylation, are clustered close to heme and the active site, while other residues studied are farther from the active site.

Active Site of P450 2B1 and Enzyme-Substrate Interactions. The active site of the P450 2B1 model, with key residues displayed, is shown in Figure 3. One can distinguish the upper part of the pocket, containing residues 114 and 290, and the lower part, with residues 478 and 480. These two groups of residues cannot interact with the substrate androstenedione simultaneously, when it is docked in a 16α - or 16β -binding orientation. The analysis of enzyme-substrate interactions was performed for these two orientations, since they reflect major products of androstenedione hydroxylation. Ile-114 located in the upper pocket interacts mainly with ring A on the β -face of androstenedione in 16α - and 16β -binding orientations (Figure 4), while Ile-290 interacts with ring A in the 16α orientation only (not shown).

³ The coordinates of the model are available from the corresponding author. E-mail address: Szklař@tonic.pharm.arizona.edu.

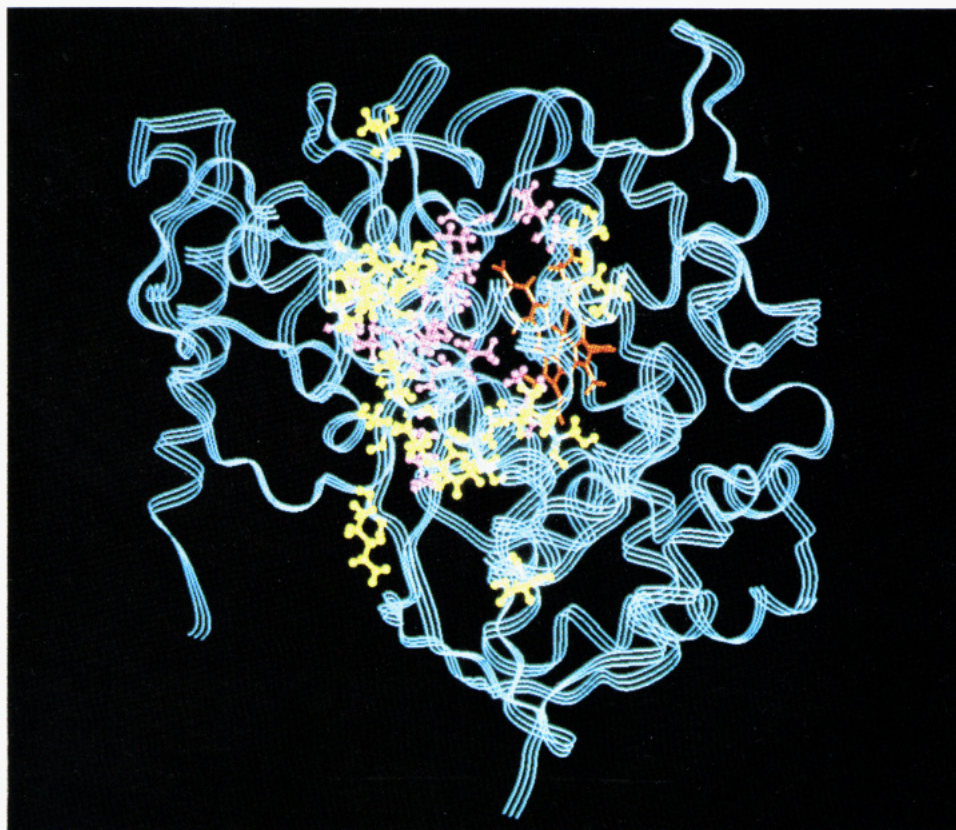


FIGURE 2: Ribbon representation of the P450 2B1 model showing the location of amino acid residues studied by site-directed mutagenesis in the 2B subfamily. Heme is shown in red, key residues are in purple, and the other residues studied are in yellow. All of these residues are listed in Table 2.

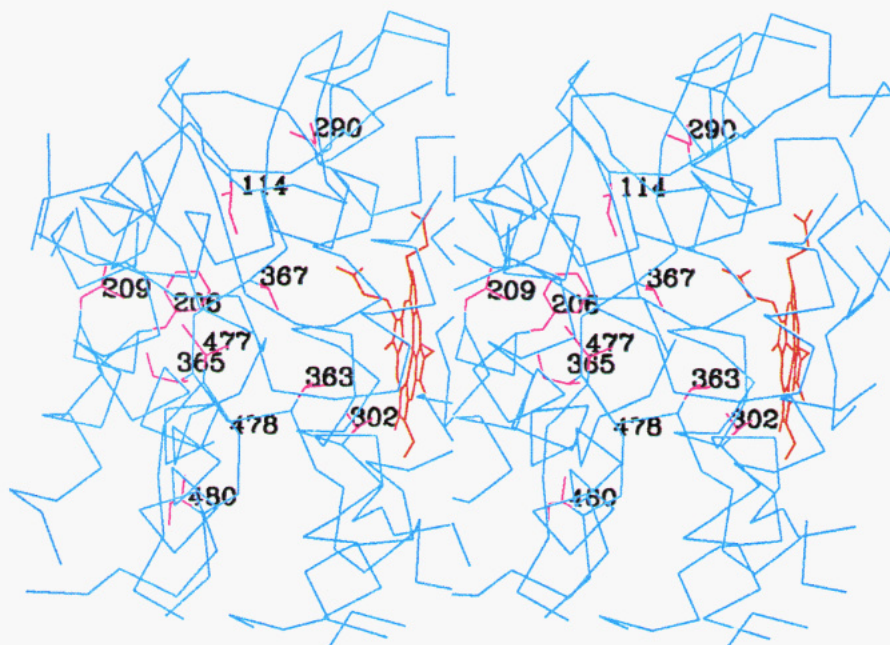


FIGURE 3: Stereoview of the active site of P450 2B1. Key residues are shown in purple, heme is in red, and the C_{α} trace is in blue.

Gly-478 is closest to C_6 of androstenedione when docked in a 16β -binding orientation (Figure 5) and to C_{19} in a 16α orientation. Phe-206 contacts the α -face when androstenedione is bound in a 16β orientation in the lower or upper pocket, and Ser-302 and Val-363 may interact with various atoms of ring D in 16α - and 16β -binding orientations in both the upper and lower pocket (Figures 4 and 5). Generally, the identity of substrate atoms in proximity to a given residue

will depend upon the particular orientation assumed by the substrate.

Interpretation of Site-Directed Mutagenesis Results. To analyze site-directed mutagenesis data, we docked a steroid substrate in various reactive binding orientations into the model of P450 2B1 in which key amino acid residues were replaced to mimic the mutants. Docking of androstenedione in 16α -, 16β -, and 15α -binding orientations confirmed key

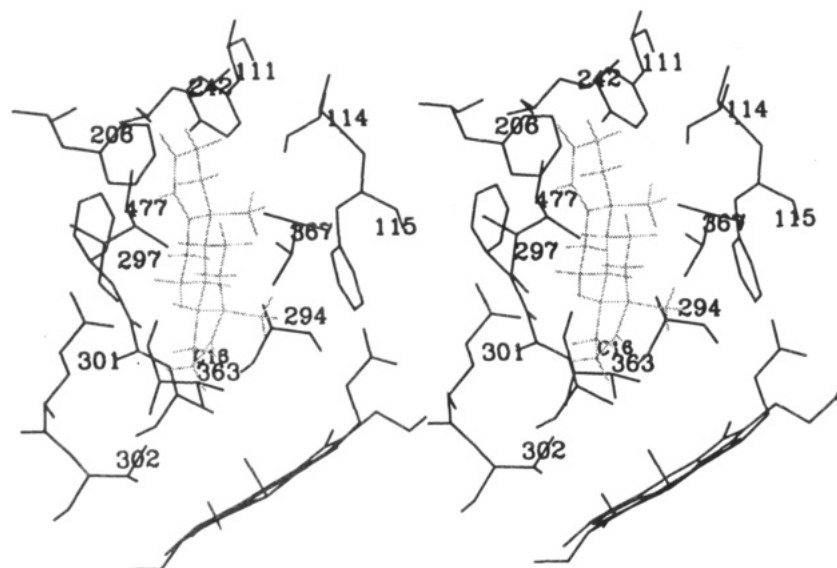


FIGURE 4: Androstenedione docked into the upper part of the binding pocket of the P450 2B1 model in a 16β -binding orientation. The substrate is shown in gray, with all hydrogens displayed.

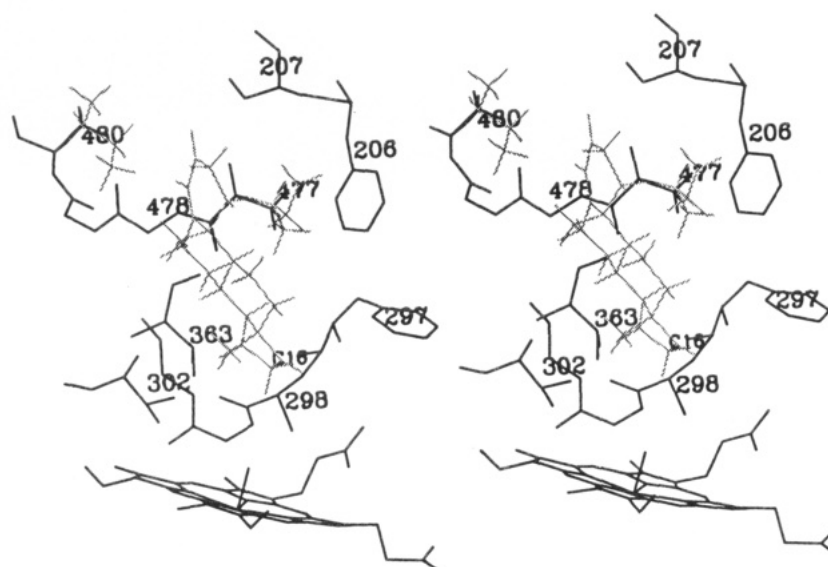


FIGURE 5: Androstenedione docked into the lower part of the binding pocket of the P450 2B1 model in a 16β -binding orientation. The side chains of Ile-477 and Ile-480, with all hydrogens displayed, are shown in gray, as is the substrate. The side chain of Ala, in black, is superimposed on Ile in both the 477 and 480 positions. Upon replacement of Ile with Ala in either of these positions, there are no longer any interactions between the substrate and the side chain, and androstenedione is not held in a 16β orientation.

roles of residues 114, 206, 290, 302, 363, and 478 (not shown), in agreement with the data and our previous model (Szklarz et al., 1994).

With the new model, we were able to explain the effect of a Val-367 \rightarrow Ala mutation, which was not possible earlier (Szklarz et al., 1994). Figure 6 shows androstenedione docked in a 6β -binding orientation in the V367A mutant. If Ala is present, the substrate can be easily accommodated in this new orientation, while the presence of a bigger Val may hinder the substrate from assuming this position. Furthermore, the substitution of Val with a bigger Leu can not only prevent 6β -hydroxylation but also impede binding of androstenedione in 16α - and 16β -binding orientations (not shown), resulting in a decrease in activity. This is in agreement with experimental data, which showed that the replacement of Val-367 with Ala conferred androgen 6β -hydroxylase activity, while the 16 -hydroxylase activity of

the V367L mutant was significantly decreased (He et al., 1994).

The effect of mutations at positions 477 and 480 is shown in Figure 5. These two residues appear to play a role in holding the substrate in a 16β -binding orientation through multiple hydrophobic interactions: Ile-477 contacts the α -face of the substrate, while Ile-480 interacts with the β -face of androstenedione. Upon mutation of either residue to Ala, the side chains are too far from the substrate for the interactions to be maintained. This may result in the increased mobility of the substrate in the active site and lack of ability of the mutant to keep androstenedione in a 16β orientation. A similar situation occurs in a 16α -binding orientation, where Ile-477 and Ile-480 interact with the β -face of the steroid and their replacement by Ala may likewise reduce the ability of the enzyme to hold the substrate in the proper orientation (not shown), which leads to a substantial decrease in 16α -hydroxylation (Table 1). Increased substrate

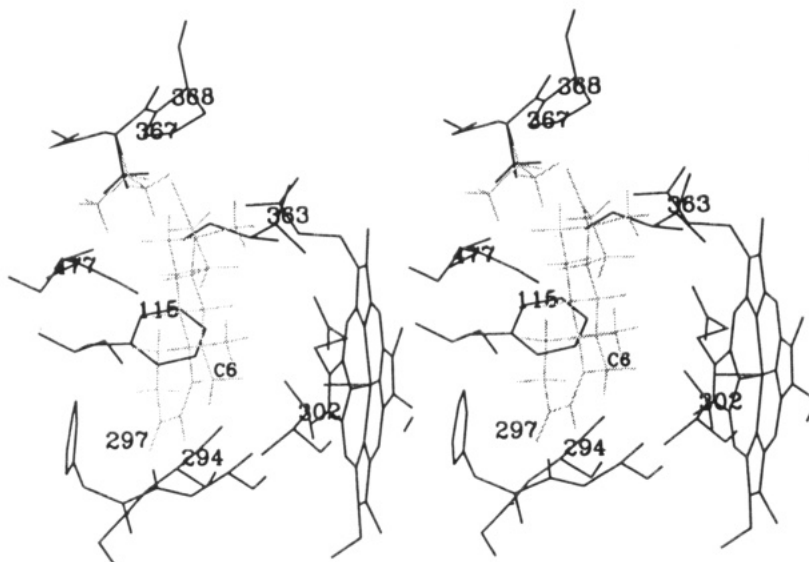


FIGURE 6: Androstenedione docked into the active site of the P450 2B1 model in a 6β -binding orientation upon replacement of Val-367 with Ala. The substrate is shown in gray, as is the side chain of Val-367 superimposed on that of Ala (black). Both residues are shown with hydrogens included. When Val is present, as in the wild-type enzyme, van der Waals overlaps occur between the substrate and the amino acid side chain, preventing androstenedione from assuming a 6β orientation.

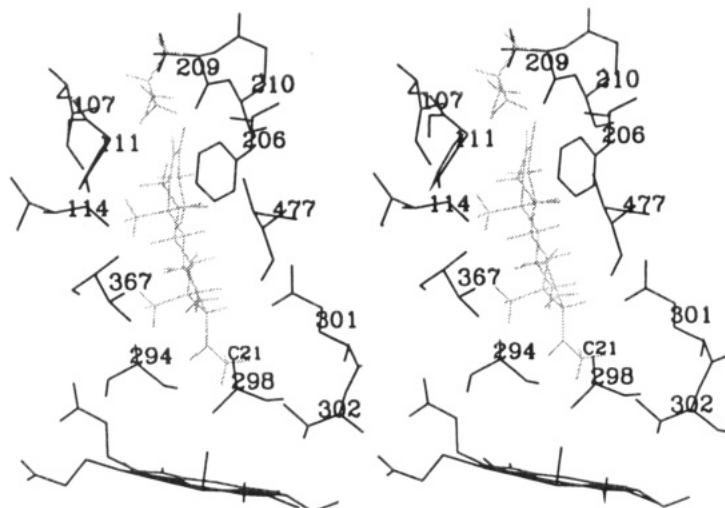


FIGURE 7: Progesterone docked into the active site of P450 2B1 in a 21-binding orientation upon replacement of Ile-209 with Ala. The side chain of Ile is shown in gray; all hydrogens are displayed, superimposed on the side chain of Ala (black). The larger Ile does not allow the substrate to assume a 21 orientation due to van der Waals overlaps.

mobility or alternate binding orientation was advanced as a probable cause of the decrease in regiospecificity of camphor hydroxylation by a P450cam Val-247 \rightarrow Ala mutant (Atkins & Sligar, 1989). Such an interpretation may also explain the lack of significant changes in hydroxylation of androstenedione by those 477 and 480 mutants in which Ile was replaced by relatively large Val and Leu residues, which can still retain hydrophobic interactions with the substrate.

Mutation of Ile-209 \rightarrow Ala caused 21-hydroxylation of progesterone, not detected in the wild-type enzyme (Table 1). Progesterone is bigger than androstenedione due to the presence of a two-carbon side chain at C₁₇. Thus, the hydroxylation of progesterone at C₂₁ requires an enlarged active site that would accommodate that side chain. The substitution of Ile with Ala allows progesterone to bind in a 21 orientation (Figure 7), while the presence of the much larger Ile would hinder the substrate from assuming this orientation.

DISCUSSION

Modeling mammalian cytochromes P450 has been considered useful when combined with experimental data (Poulos, 1991; Laughton et al., 1993). This approach has been applied by Graham-Lorence et al. (1991), who combined modeling and site-directed mutagenesis to study structure–function relationships of aromatase, and by Iwasaki et al. (1993, 1994), who modeled the active site of P450 2A4 to interpret enzyme–substrate interactions and the role of key residue 209. Recently, Zhou et al. (1994) tested the molecular model of aromatase (Laughton et al., 1993) using site-directed mutagenesis coupled with inhibitor studies and demonstrated how experimental studies may help to correct the model. In our previous work (Szklař et al., 1994), we built a model of P450 2B1 based on P450cam and showed its usefulness for interpretation of site-directed mutagenesis results. Moreover, the model also suggested other residues likely to be essential for enzyme function.

Although not all residues postulated by that model proved to be important modulators of P450 2B1 activity with androstenedione or progesterone, we identified three additional key positions, 209, 477, and 480, two of which, 209 and 480, were not included in the six substrate recognition sites (SRSs) proposed by Gotoh (1992). So far, only five SRSs, SRS-1, SRS-2, SRS-4, SRS-5, and SRS-6, have been confirmed experimentally in P450 2B1 (He et al., 1994). The analysis of known crystal structures and multiple sequence alignment of various P450s suggest that, in addition to sequence hypervariability of the SRSs, there is spacial hypervariability in SRS-1 (B' helix), SRS-2 (C-terminal region of the F helix), and SRS-3 (N-terminal region of the G helix). Moreover, SRS-3 is not likely to be present in most P450s, including mammalian enzymes (Hasemann et al., 1995). This is supported by site-directed mutagenesis data, which showed that the substitution of SRS-3 residues 234 (Hasler et al., 1994) and 236 (He et al., 1995) did not affect the activity of P450 2B11 and 2B1, respectively. Likewise, our present model does not predict any role for residues 234–241, which constitute SRS-3 in 2B enzymes. Thus, although Gotoh's hypothesis has served well in identification of key amino acid residues, one must exercise some caution when extending the SRS concept to eukaryotic P450s. Modeling may have a substantial advantage here, since it relies on the three-dimensional structure, and the possible role for residues of interest can be inferred from docking of various substrates into the active site.

In modeling a new structure, the sequence alignment as well as the choice of reference proteins is of crucial importance. Since until recently only one P450 structure, that of P450cam, was available, all earlier models used P450cam as the only reference protein (Zvelebil et al., 1991; Vijayakumar & Salerno, 1992; Koymans et al., 1993; Laughton et al., 1993; Braatz et al., 1994; Szklaarz et al., 1994). Recently, the crystal structures of P450 BM-3 and P450cam were utilized to model thromboxane synthase, and the former structure proved to be a better template for the synthase (Ruan et al., 1994). In the case of cytochrome P450 2B1, the sequence identity with any of the solved cytochromes is very low (below 20%), and the choice of the reference protein is difficult. Moreover, docking of androstenedione into known structures has shown that any of them may be a suitable template for modeling and led us to employ consensus modeling methods, in which all reference protein coordinates are utilized to build a model. The basis for the model building was therefore the structure-based alignment of P450 2B1, P450cam, P450 BM-3, and P450terp. This type of alignment is more accurate than that produced from sequence conservation alone, particularly in the regions of low sequence identity (Hasemann et al., 1995). Furthermore, the regions with reasonable sequence conservation need not always superimpose in space. The structure-based alignment establishes overall P450 fold found in known structures, which can be extended to other cytochromes P450 (Hasemann et al., 1995). Our alignment of P450 2B1 is essentially the same as that proposed by Hasemann et al. (1995), with minor differences such as the alignment of helix B' and the B'–C loop, sheet $\beta 3-1$, helix F, or sheet $\beta 5-1$.

The refinement of our alignment utilized a novel approach based on site-directed mutagenesis data for cytochromes P450 2B and docking of the P450 2B1 substrate androstenedione into the active site of the known structures.

Enzymes within the 2B subfamily display high sequence identity and thus should have very similar structures. Consequently, the data from site-directed mutagenesis of one 2B enzyme should be applicable to another, as was found experimentally in the case of residues 114 and 363 of P450 2B1 (Halpert & He, 1993; He et al., 1994; Luo et al., 1994) and 2B11 (Hasler et al., 1994).⁴ Since our refinement procedure relies heavily on experimental data, it should lead to the optimal structure consistent with those data. This approach may be of particular advantage for modeling regions of high variability among known P450s, such as helices B', F, or G, where the sequence alignment remains uncertain. Similar methods might also be employed to model other P450 enzymes for which site-directed mutagenesis data are available.

It has been demonstrated that related cytochromes of the P450 2 family share the same substrate recognition sites, which should be reflected in their three-dimensional structures. Many of these enzymes have been extensively studied by site-directed mutagenesis, often in conjunction with sequence alignment with P450cam and/or P450 BM-3. Due to the overall conservation of the P450 fold (Hasemann et al., 1995), there is no uncertainty as to the location of key residues which are part of highly conserved structural elements, such as helix I (Imai & Nakamura, 1989; Hanioka et al., 1992; Fukuda et al., 1993; Hasler et al., 1994; He et al., 1994). In other regions of the active site, both the alignment and its structural implications are a question of some debate. The region of helix B' and the B'–C loop has been studied in the 2A subfamily (Lindberg & Negishi, 1989; Iwasaki et al., 1994), 2B subfamily (Aoyama et al., 1989; Halpert & He, 1993; Hasler et al., 1994), and 2C subfamily (Straub et al., 1993a,b, 1994; Richardson & Johnson, 1994). The alignments proposed for this region in P450 2C (Straub et al., 1994; Richardson & Johnson, 1994) differ from the alignment we used (Figure 1), but since this region is hypervariable in crystal structures, we can expect it to possess a unique topology. In our model, the structure of this region is consistent with the data from site-directed mutagenesis of cytochrome P450 2B1 and the postulated role of residue 114, as well as the equivalent residue 113 in 2C3 (Straub et al., 1993a,b). The C-terminal end of helix F contains key residue 209 in P450 2A4 and 2A5 (Lindberg & Negishi, 1989; Juvonen et al., 1991; Negishi et al., 1992; Iwasaki et al., 1993) equivalent to residue 206 in P450 2B1 (Luo et al., 1994; He et al., 1994). The alignment of this helix in our present model is the same as used by Iwasaki et al. (1993), who mapped this residue to Met-184 of P450cam, as described in Results. Another interesting region is the K- $\beta 1-4$ loop and the $\beta 1-4$ sheet containing several key residues, such as residue 365 in P450 2A4/2A5 (Lindberg & Negishi, 1989), residues 363 and 367 in P450 2B1 and 2B11 (Luo et al., 1994; He et al., 1994; Hasler et al., 1994), or residues 359 and 364 in the 2C subfamily (Kaminsky et al., 1992; Hsu et al., 1993). The alignment of 2C3 proposed by Richardson and Johnson (1994) places Thr-364, which is equivalent to residue 366 of P450 2B1, at the position corresponding to Phe-331 of P450 BM-3 and Asp-297 of P450cam, which leads to a one-residue shift when compared

⁴ This also is true for residues 114, 363, and 367 in P450 2B4/2B5, as suggested by recent site-directed mutagenesis results (Vicki Burnett, manuscript in preparation).

to our alignment. In our model, the region containing residues 364–366 forms a loop which allows key residues 363 and 367 to interact with the steroid substrate. Residue 367 is essential for 6 β -hydroxylation of steroids in P450 2B1 (He et al., 1994) and 2B5,⁴ as shown in Figure 6. Residue 366 is also close to the substrate, and its mutation may likewise effect steroid hydroxylation, as observed for the equivalent residue 364 in 2C3 (Richardson & Johnson, 1994).

Docking of the substrate into the active site of the enzyme model has been successfully utilized to interpret enzyme–substrate interactions and the possible role of key amino acid residues (Graham-Lorence et al., 1991; Zvebil et al., 1991; Iwasaki et al., 1993, 1994; Koymans et al., 1993; Laughton et al., 1993; Szklarz et al., 1994; Zhou et al., 1994). Our previous studies with a P450 2B1 model showed that hydrophobic interactions are mainly responsible for binding the substrate in the active site and that there may be several substrate binding orientations (Szklarz et al., 1994). The site-directed mutagenesis results were also satisfactorily explained for key residues 114, 290, 302, 363, and 478. However, the location of other key residues was not correct. In the present studies, the positions of residues 206, 209, and 367 were changed, and the results from docking of steroid substrates are now in agreement with site-directed mutagenesis data. Thus, Phe-206 interacts with androstenedione in various 16 α and 16 β orientations (see Figures 4 and 5), while residue 209 may only effect binding of progesterone in a 21 orientation (Figure 7). Furthermore, Val-367 is now placed in a position in which it may effect 6 β -hydroxylation of androstenedione (Figure 6). Other residues, such as 100, 111, and 205, which were predicted to effect steroid hydroxylation according to our earlier model, cannot directly interact with the substrate, in agreement with the data. Therefore, the present model is superior to the previous one, since it is consistent with all available site-directed mutagenesis results.

Our analysis of the 11 mutants studied in the present investigation indicated that only three of them, at positions 209, 477, and 480, affect the metabolism of androstenedione or progesterone (Table 1). There was some variation in the activities of other mutants, possibly due to an effect of a particular substitution upon the volume of the active site, e.g., in the case of residues 111 or 291. Although they may be within 4 Å distance from the substrate, these residues cannot interact with the steroid directly due to a “screen” effect of other residues. For example, residue 111 is unable to interact directly with androstenedione bound in a 16 β orientation due to the presence of side chains of residues 114 and 206, among others (Figure 4). However, if residues 111 or 291 are mutated to smaller or larger residues, they may influence conformations of their closest neighbors in contact with the substrate, and this can lead to a slight decrease or increase in activity without changing the ratios of metabolites or with only a minor change in ratios depending upon the residue.

Our present studies support the validity of modeling P450 structure when combined with site-directed mutagenesis data. Such an approach may provide valuable insight into enzyme regio- and stereospecificity and lead to predictions, which can be verified experimentally. This can be of great advantage in the rational design of drugs and inhibitors, as well as enzymes with altered substrate specificity.

ACKNOWLEDGMENT

The authors thank Dr. Rick Ornstein and Dr. Mark Paulsen for helpful discussions and the use of the facilities at the Environmental Molecular Science Laboratory, Pacific Northwest Laboratory, Richland, WA, to run CONSENSUS calculations. All other molecular modeling studies were performed in the Molecular Modeling Facility of the Southwest Environmental Health Sciences Center (SWEHSC) at the University of Arizona, Tucson, AZ (ES06694). Tandem mass spectrometry was carried out in the Analytical Core of the SWEHSC by Dr. Daniel Liebler and Dr. Thomas McClure. We also thank Dr. Rick Ornstein, Dr. William Remers, and Dr. Vicki Burnett for reviewing the manuscript.

REFERENCES

- Aoyama, T., Korzekwa, K., Nagata, K., Adesnik, M., Reiss, A., Lapenson, D. P., Gillette, J., Gelboin, H. V., Waxman, D. J., & Gonzalez, F. J. (1989) *J. Biol. Chem.* 264, 21327–21333.
- Atkins, W. M., & Sligar, S. G. (1989) *J. Am. Chem. Soc.* 111, 2715–2717.
- Born, S. L., John, G. H., Harlow, G. R., & Halpert, J. R. (1995) *Drug Metab. Dispos.* 23, 702–707.
- Bowie, J. U., Luthy, R., & Eisenberg, D. (1991) *Science* 253, 164–170.
- Braatz, J. A., Bass, M. B., & Ornstein, R. L. (1994) *J. Comput.-Aided Mol. Des.* 8, 607–622.
- Cupp-Vickery, J. R., & Poulos, T. L. (1995) *Struct. Biol.* 2, 144–153.
- Fukuda, T., Imai, Y., Komori, M., Nakamura, M., Kusunose, E., Satouchi, K., & Kusunose, M. (1993) *J. Biochem.* 113, 7–12.
- Gotoh, O. (1992) *J. Biol. Chem.* 267, 83–90.
- Graham-Lorence, S., Khalil, M. W., Lorence, M. C., Mendelson, C. R., & Simpson, E. R. (1991) *J. Biol. Chem.* 266, 11939–11946.
- Guengerich, F. P. (1993) *Drug Metab. Dispos.* 21, 1–6.
- Halpert, J. R., & He, Y.-A. (1993) *J. Biol. Chem.* 268, 4453–4457.
- Hanioka, N., Gonzalez, F. J., Lindberg, N. A., Liu, G., Gelboin, H. V., & Korzekwa, K. R. (1992) *Biochemistry* 31, 3364–3370.
- Hasemann, C. A., Ravichandran, K. G., Peterson, J. A., & Deisenhofer, J. (1994) *J. Mol. Biol.* 236, 1169–1185.
- Hasemann, C. A., Kurumbail, R. G., Boddupalli, S. S., Peterson, J. A., & Deisenhofer, J. (1995) *Structure* 3, 41–62.
- Hasler, J. A., Harlow, G. R., Szklarz, G. D., John, G. H., Kedzie, K. M., Burnett, V. L., He, Y. A., Kaminsky, L. S., & Halpert, J. R. (1994) *Mol. Pharmacol.* 46, 338–345.
- He, Y.-A., Balfour, C. A., Kedzie, K. M., & Halpert, J. R. (1992) *Biochemistry* 31, 9220–9226.
- He, Y.-A., Luo, Z., Klekotka, P. A., Burnett, V. L., & Halpert, J. R. (1994) *Biochemistry* 33, 4419–4424.
- He, Y. Q., He, Y.-A., & Halpert, J. R. (1995) *Chem. Res. Toxicol.* 8, 574–579.
- Hsu, M.-H., Griffin, K. J., Wang, Y., Kemper, B., & Johnson, E. F. (1993) *J. Biol. Chem.* 268, 6939–6944.
- Imai, Y., & Nakamura, M. (1989) *Biochem. Biophys. Res. Commun.* 158, 717–722.
- Iwasaki, M., Darden, T. A., Pedersen, L. G., Davis, D. G., Juvonen, R. O., Sueyoshi, T., & Negishi, M. (1993) *J. Biol. Chem.* 268, 759–762.
- Iwasaki, M., Darden, T. A., Perker, C. E., Tomer, K. B., Pedersen, L. G., & Negishi, M. (1994) *J. Biol. Chem.* 269, 9079–9083.
- John, G. H., Hasler, J. A., He, Y.-A., & Halpert, J. R. (1994) *Arch. Biochem. Biophys.* 314, 367–375.
- Johnson, E. F. (1992) *Trends Pharmacol. Sci.* 13, 122–126.
- Juvonen, R., Iwasaki, M., & Negishi, M. (1991) *J. Biol. Chem.* 266, 16431–16435.
- Kaminsky, L. S., de Morais, S. M. F., Faletto, M. B., Dunbar, D. A., & Goldstein, J. A. (1992) *Mol. Pharmacol.* 43, 234–239.
- Kedzie, K. M., Balfour, C. A., Escobar, G. Y., Grimm, S. W., He, Y.-A., Pepperl, D. J., Regan, J. W., Stevens, J. C., & Halpert, J. R. (1991) *J. Biol. Chem.* 266, 22515–22521.

- Korzekwa, K. R., & Jones, J. P. (1993) *Pharmacogenetics* 3, 1–18.
- Koymans, L. M. H., Vermeulen, N. P. E., Baarslag, A., & Donne-Op den Kelder, G. M. (1993) *J. Comput.-Aided Mol. Des.* 7, 281–289.
- Laughton, C. A., Zvelebil, M. J. J. M., & Neidle, S. (1993) *J. Steroid Biochem. Mol. Biol.* 44, 399–407.
- Lindberg, R. L. P., & Negishi, M. (1989) *Nature* 227, 632–634.
- Luo, Z., He, Y.-A., & Halpert, J. R. (1994) *Arch. Biochem. Biophys.* 309, 52–57.
- Luthy, R., Bowie, J. U., & Eisenberg, D. (1992) *Nature* 365, 83–85.
- Matsunaga, E., Zeugin, T., Zanger, U. M., Aoyama, T., Meyer, U. A., & Gonzalez, F. J. (1990) *J. Biol. Chem.* 265, 17197–17201.
- Nash, T. (1953) *Biochem. J.* 55, 416–421.
- Negishi, M., Iwasaki, M., Juvonen, R. O., & Aida, K. (1992) *J. Steroid Biochem. Mol. Biol.* 43, 1031–1036.
- Nelson, D. R., & Strobel, H. W. (1988) *J. Biol. Chem.* 263, 6038–6050.
- Nelson, D. R., & Strobel, H. W. (1989) *Biochemistry* 28, 656–660.
- Paulsen, M. D., & Ornstein, R. L. (1991) *Proteins* 11, 184–204.
- Paulsen, M. D., & Ornstein, R. L. (1992) *J. Comput.-Aided Mol. Des.* 6, 449–460.
- Poulos, T. L. (1991) *Methods Enzymol.* 206, 11–30.
- Poulos, T. L., Finzel, B. C., Gunsalus, I. C., Wagner, G. C., & Kraut, J. (1985) *J. Biol. Chem.* 260, 16122–16130.
- Poulos, T. L., Finzel, B. C., & Howard, A. (1987) *J. Mol. Biol.* 195, 687–700.
- Ravichandran, K. G., Boddupalli, S. S., Hasemann, C. A., Peterson, J. A., & Deisenhofer, J. (1993) *Science* 261, 731–736.
- Richardson, T. H., & Johnson, E. F. (1994) *J. Biol. Chem.* 269, 23937–23943.
- Ruan, K.-H., Milfeld, K., Kulmacz, R. J., & Wu, K. K. (1994) *Protein Eng.* 7, 1345–1351.
- Straub, P., Johnson, E. F., & Kemper, B. (1993a) *Arch. Biochem. Biophys.* 306, 521–527.
- Straub, P., Lloyd, M., Johnson, E. F., & Kemper, B. (1993b) *J. Biol. Chem.* 268, 21997–22003.
- Straub, P., Lloyd, M., Johnson, E. F., & Kemper, B. (1994) *Biochemistry* 33, 8029–8034.
- Swinney, D. C., Ryan, D. E., Thomas, P. E., & Levin, W. (1987) *Biochemistry* 26, 7073–7083.
- Szklař, G. D., Ornstein, R. L., & Halpert, J. R. (1994) *J. Biomol. Struct. Dyn.* 12, 61–78.
- Vijayakumar, S., & Salerno, J. C. (1992) *Biochim. Biophys. Acta* 1160, 281–286.
- Waxman, D. J. (1988) *Biochem. Pharmacol.* 37, 71–84.
- Zhou, D., Cam, L. L., Laughton, C. A., Korzekwa, K. R., & Chen, S. (1994) *J. Biol. Chem.* 269, 19501–19508.
- Zvelebil, M. J. J. M., Wolf, C. R., & Sternberg, M. J. E. (1991) *Protein Eng.* 4, 271–282.

BI9509412